ГЕОМОРФОЛОГИЯ, 2022, том 53, № 3, с. 83–95

СЕДИМЕНТОЛОГИЯ, ПАЛЕОГЕОКРИОЛОГИЯ, ПАЛЕОГИДРОЛОГИЯ

УДК 551.89:556.555.6 (470.12)

ДИНАМИКА ОСАДКОНАКОПЛЕНИЯ В ОЗЕРЕ БЕЛОМ (ВОЛОГОДСКАЯ ОБЛАСТЬ, СЕВЕРО-ЗАПАД РОССИИ) С ПОЗДНЕЛЕДНИКОВЬЯ ДО СРЕДНЕГО ГОЛОЦЕНА

© 2022 г. Д. О. Садоков[1,2,*], Т. В. Сапелко[3], М. Меллес[4], Г. Б. Федоров[2,5]

[1] *Дарвинский государственный природный биосферный заповедник, Череповец, Россия*

[2] *Санкт-Петербургский государственный университет, Институт наук о Земле, Санкт-Петербург, Россия*

[3] *Институт озероведения РАН, СПб ФИЦ РАН, Санкт-Петербург, Россия*

[4] *Университет Кёльна, Институт геологии и минералогии, Кёльн, Германия*

[5] *Арктический и Антарктический научно-исследовательский институт, Санкт-Петербург, Россия*

*****E-mail: dmitriisadokov@gmail.com*

Поступила в редакцию 30.03.2022 г.
После доработки 10.04.2022 г.
Принята к публикации 15.04.2022 г.

Представлены первые результаты исследований озерных отложений северной части Молого-Шекснинской низменности с использованием рентгенофлуоресцентного сканирования высокого разрешения и AMS датирования, дополненных рентгенофазовым анализом, измерением общего органического углерода, гранулометрического состава и магнитной восприимчивости. Изменения режима седиментации в течение позднеледниковья и раннего голоцена были соотнесены с относительным количеством аллогенного и аутигенного вещества в отложениях, выявленного на основании анализа минерального и элементного состав неорганической фракции. Интервалы, отличающиеся низкой аллогенной аккумуляцией, были отмечены ~14.0 и ~13.0 кал. тыс. л. н., с перерывами на кратковременные события, связанные с повышенным минерагенным сносом и низкой органогенной аккумуляцией ~13.7, 13.1 и 11.5 кал. тыс. л. н. Отмеченные интервалы хронологически соответствуют позднеледниковым климатостратиграфическим подразделениям, выделенным для Северной Атлантики. Резкий всплеск органогенной седиментации ~11.7 кал. тыс. л. н. рассматривается как индикатор потепления в раннем голоцене. Выраженные в геохимических показателях регрессия и изоляция мелководных озер от крупного палеоводоема отмечаются с ~12.0 кал. тыс. л. н. Во время позднего дриаса и раннего голоцена режим седиментации во многом зависел от колебаний уровня водоема, который претерпел окончательное дренирование к ~11.0 кал. тыс. л. н.

Ключевые слова: озерное осадконакопление, геохимия, аллерёд, поздний дриас

DOI: 10.31857/S0435428122030142

1. INTRODUCTION

The margins and retreat dynamics of the Late Valdai (Late Weichselian) glaciation in the Mologa-Sheksna Lowland (MSL) have been long debated, with different reconstructions of the ice sheet limits (Lunkka et al., 2001; Astakhov et al., 2016; Hughes et al., 2016) and positions of proglacial lakes (Moskvitin, 1947; Pozdnechetvertichnaya..., 1974; Gey, 2000). First comprehensive geological surveys commenced in the northern MSL as early as the 1960-s and 1970-s (Mokrienko et al., 1976), and numerous studies of the deglaciation chronology and the related palaeohydrology were performed in the adjacent regions and the surroundings during the last decades (Lunkka et al., 2001; Saarnisto, Saarinen, 2001; Mangerud et al., 2004; Svendsen et al., 2004; Sapelko et al., 2006; Velichko, Faustova, 2009; Astakhov et al., 2016; Hughes et al., 2016). Nevertheless, little reliable evidence is currently available on the actual landscape evolution in the northern MSL. This is mainly due to a small amount of dated records in the area, which caused certain misinterpretation, of the Last Glacial Maximum (LGM) limits (Chebotaryova, 1962; Lunkka et al., 2001), as well as the spatial and temporal distribution of the palaeolakes (Khavin, 1962; Auslender, 1967; Faustova et al., 1969; Gey, 2000). Since most of the LGM and Late-Glacial marginal landforms of the northern MSL are believed to be completely eroded by fluvioglacial streams of the transgressive Vepsian glacial stage (Mokrienko et al., 1976), it is particularly relevant to build an accurate reconstruction from undisturbed continuous lacustrine sequences, some of which were reported to reach down to mid-Late-Glacial (Mokrienko et al., 1976).

Fig. 1. Lake Beloye geographical position on the map of northwestern Russia and northern Europe (a) and in the Babaevo district, Vologda region (b). White circle marks the site of the coring.

Рис. 1. Географическое положение оз. Белого на карте северо-запада России и северной Европы (a) и Бабаевского района Вологодской области (b). Белым кружком отмечено место бурения.

In an attempt to unravel the Late-Glacial to Middle Holocene hydrological and sedimentary dynamics in the light of the known palaeoclimatic development, geochemical, granulometric, mineralogical and geochronological analyses were performed on the sediment record from lake Beloye, northern MSL (fig. 1). Of these analyses, continuous, high-resolution X-ray fluorescence scanning (XRF) and AMS radiocarbon dating, which are recognized as effective tools in palaeolimnology (Paleolimnology..., 2003; Davies et al., 2015), were for the first time employed on lacustrine deposits from the MSL.

2. STUDY SITE

Lake Beloye (59.379° N, 35.626° E) is located in the Vologda region, Babaevo district (northwestern Russia), 15 km west from the town Babaevo (fig. 1). The lake lies at 150.5 m above sea level (a.s.l.), has an average depth 1.5 m and covers an area of 1.26 km^2. It is located between two large bogs (fig. 1), with the southern one been partially drained by several ditches. The watershed of the lake covers 50 km^2.

The lake belongs to the Kolp river basin, which is the tributary of river Suda. Bogs and mires occupy up to 60–75% of the interfluve area of rivers Mologa and Suda, and southern taiga landscapes are typically widespread over the unbogged plain (Maksutova, Vorobyov, 2007). Quaternary glacial and limnoglacial deposits comprise the upper 4–6 meters of the geologic profile (Mokrienko et al., 1976; Igolkina, 1985b), underlain by Carboniferous dolomites and limestones (Igolkina, 1985a). Holocene peat deposits are widespread over the flat terrain.

Lake Beloye is located in the very periphery of the MSL, in the transient zone between Kolp moraine plain and Mologa-Suda lowland. The boundary between the geomorphological zones is determined according to gradual change of the dominant landforms, i.e. lacustrine-glacial plains in the south-east changed by moraine-sandur hummocky relief in the northwest (Mokrienko et al., 1976).

3. MATERIALS AND METHODS

Lake sediment samples were obtained with a Russian corer (chamber length 1 m, inside diameter 5 cm). The water depth was 178 cm in the place of coring (from the ice surface). The total length of the extracted column was 409 cm. The cores were sub-sampled by every 2 cm after x-ray fluorescence scanning (see subsection 3.2).

X-ray fluorescence (XRF) scanning was performed non-destructively using ITRAX XRF Core Scanner (Cox Analytical Systems) (Cr-anode tube, 30 kV, 55 mA, dwell time 5 sec, step size 2 mm). Results were obtained as units of the reflection intensity – counts per second. Magnetic susceptibility (χ) was measured with the Muti-Sensor Core Logger (Geotek Analytical Systems).

Quantitative XRF measurements of Fe_2O_3, MnO and TiO_2 concentrations in 60 dried and grounded samples were conducted on the “Spectroscan MAX” with crystal-analyzer LiF (200) (40 kV, 0.1 mA).

After the cores were sub-sampled, each segment was weighed before and after freeze-drying in order to determine water content (WC) of the sediments.

Table 1. AMS dating results
Таблица 1. Результаты AMS датирования

Lab index ($IGAN_{AMS}$)	Depth, cm	Sample matter	^{14}C yr, BP (1σ)	Cal. yr BP
8051	330	plant fossils	4590 ± 30	5314 ± 30
8050*	463	TOC	7530 ± 40	8352 ± 40
6364	473	TOC	10 085 ± 30	11 668 ± 30
8049	503	TOC	10 670 ± 30	12 702 ± 30
8048	529	TOC	10 930 ± 35	12 821 ± 35
8047	582	TOC	12 260 ± 45	14 177 ± 45

* – value excluded from age-depth model in rBacon (not used for the accumulation rate calculation).

Total organic carbon (TOC) content was measured on Dimatoc 2000 (Dimatec Analysentechnik GmbH) in 203 samples after freeze-drying and grounding.

Phase composition of the sediment was determined using powder x-ray diffraction (XRD) on the diffractometer Bruker "D2 Phaser" (Co-anode, 30 kV, 10 mA, angles range 5°–75°, scanning step size 0.02°, exposition in each point 0.7 seconds) for 21 dried and grounded samples.

Grain-size (GS) was studied for 24 samples using laser diffractometer Mastersizer 3000 (for particles <1 mm) and represented as Dx(50) median values. The samples previously had been dried under 105°C and sieved to the fraction size <1 mm.

A total of 6 samples comprised of organic fossils and muds were used for age determination at the Laboratory of the Radiocarbon Dating and Electronic Microscopy (Institute of Geography RAS) using accelerated mass-spectrometry (AMS^{14}C) (table 1). The obtained ^{14}C ages were calibrated using IntCal20 calibration curve (Reimer et al., 2020). An age-depth model was generated in R software ('rbacon' package) (fig. 2), with the use of Bayesian inference (Blaauw, Christen, 2019).

Optical studies (mesomorphological microanalysis) of organic and mineral components in 20 dried samples was performed on the stereomicroscope Leica M205C.

Principal component analysis (PCA) was applied to the data rows (Si, Fe, Ca, K, Ti, TOC, GS, WC, χ, Mn/Fe, Si/Ti) using R program (packages 'FactoMineR', 'factoextra' and 'missMDA') (Husson et al., 2019; Husson, Josse, 2020; Kassambara, Mundt, 2020).

4. RESULTS

4.1. Lithology and core architecture. The whole studied sequence is roughly composed of three sections, where the lowermost parts (fig. 3) are represented by finely laminated greenish-brown sandy silt, and the upper zone is represented by dark brown organic muds. Sections II and III are divided by a marked transition horizon that features characteristic alterations of color, texture and fraction composition. Plant fossils (roots and seeds) are observed frequently in the upper muddy section.

4.2. Chronology. Six values of radiocarbon age were obtained in total for the studied sediment sequence (table 1). Three of them are attributed to the lowermost 100 cm section of finely laminated silt, two values mark the bottom of muddy sediments, one dating was performed for the middle part of the upper muddy section. Age-depth modeling performed in R (fig. 2) showed value 8352 ± 40 cal. ka BP (depth 463 cm) to be invalid, not corresponding to other age values used in the Bayesian model.

4.3. Elemental composition and physical properties. Highest intensity of Fe, K, Ti, Si and Ca signal (fig. 3) is recorded at the depth 587–530 cm, accompanied by large oscillations amplitude over the general decreasing trend. Several notable synchronous drops of Fe, K, Ti, Si and Ca content are recorded at the depths 578–574 cm, 545 cm and 539–526.5 cm. An extensive increase of these elements content is registered at the depth 530–485 cm. The elements content abruptly drops at the depth 485–460 cm, with the fluctuation amplitude also declining at this interval. The elements content remains critically low from the depth 460 cm until the sediments upper border.

Si/Ti and Mn/Fe ratios (fig. 4) show quite low values without any expressed fluctuations at the depths 587–486 cm. From 475 to 465 cm Mn/Fe values gradually increase, while Si/Ti values decline. Then at the depth 475–178 cm both ratios demonstrate higher frequency rate with the larger amplitude. Average Mn/Fe values rise up to 0.4. A series of repeated peak values of Si/Ti and Mn/Fe ratios are observed at the depth intervals 311–309, 300–269, 243–235 and 198–178 cm.

Low figures of magnetic susceptibility (χ) (fig. 4) under 4 SI × 10^{-5} are observed for most of the studied sequence, with distinctive drops at the depth intervals 578–574 and 539–526.5 cm. χ decreases by two times in the upper section of muddy sediments, with several short splashes, which are most likely due to the laboratory error.

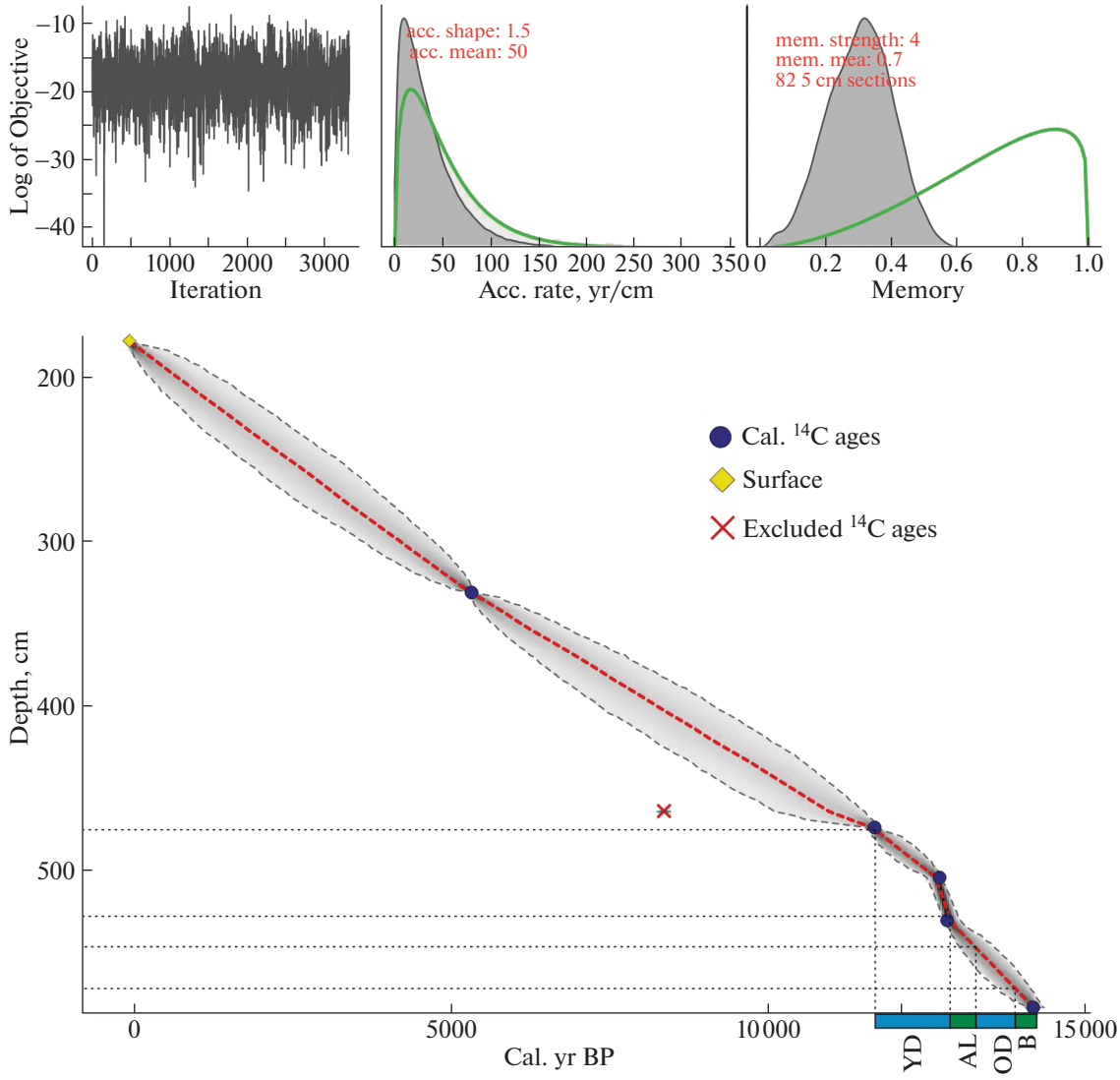

Fig. 2. Bayesian age-depth model for the Lake Beloye studied sediment sequence basing on 5 AMS dates, built with the use of 'Bacon' package in R. Modelled age-depth limits of chronozones: YD – Younger Dryas, AL – Allerød, OD – Older Dryas, B – Bølling.

Рис. 2. Байесовская возрастная модель для изученной колонки отложений оз. Белого, выполненная с использованием 5 AMS датировок в пакете 'Bacon' в R. Индексами условно отмечены смоделированные возрастные границы хронозон: YD – поздний дриас, AL – аллерёд, OD – средний дриас, B – бёллинг.

The lowest values of water content (WC) of the sediments (22%) are recorded at the depth 587–582 cm, which increase upcore to 60–70% by the depth 540–530 cm (fig. 4). After a slight drop to 51% at the depth 489 cm, WC steadily rises upcore to 92%.

4.4. Total organic carbon. The lowest figures of total organic carbon (TOC) content (2–8%) are attributed to the interval 587–547 cm (fig. 4), which is followed by a marked increase to 19% at the depth 539–526.5 cm. A rapid rise of the TOC content (up to 53%) is recorded within the zone of the transition to the muddy sediments (477–459 cm). TOC values maintain constant around 51% until the upper sediments border.

4.5. Grain size. Most frequent oscillations of grain-size median values are recorded in the lowermost part of the sequence, with a series of particle size shifts from 65 μm to 138 μm attributed to the depth 555–530 cm (fig. 4). The values sustain around 110 μm beginning from the depth 475 cm, except the interval around 297 cm, where median particle size drops down to 77 μm.

4.6. Mineral composition. The share of quartz composes around 50% of the whole inorganic matter of the sediments (fig. 5). Feldspar minerals also show enhanced abundance (around 20%) at the depth 587–527 cm. A notable peak in quartz distribution (89%) is registered at the level 441 cm. Soon after that, at the

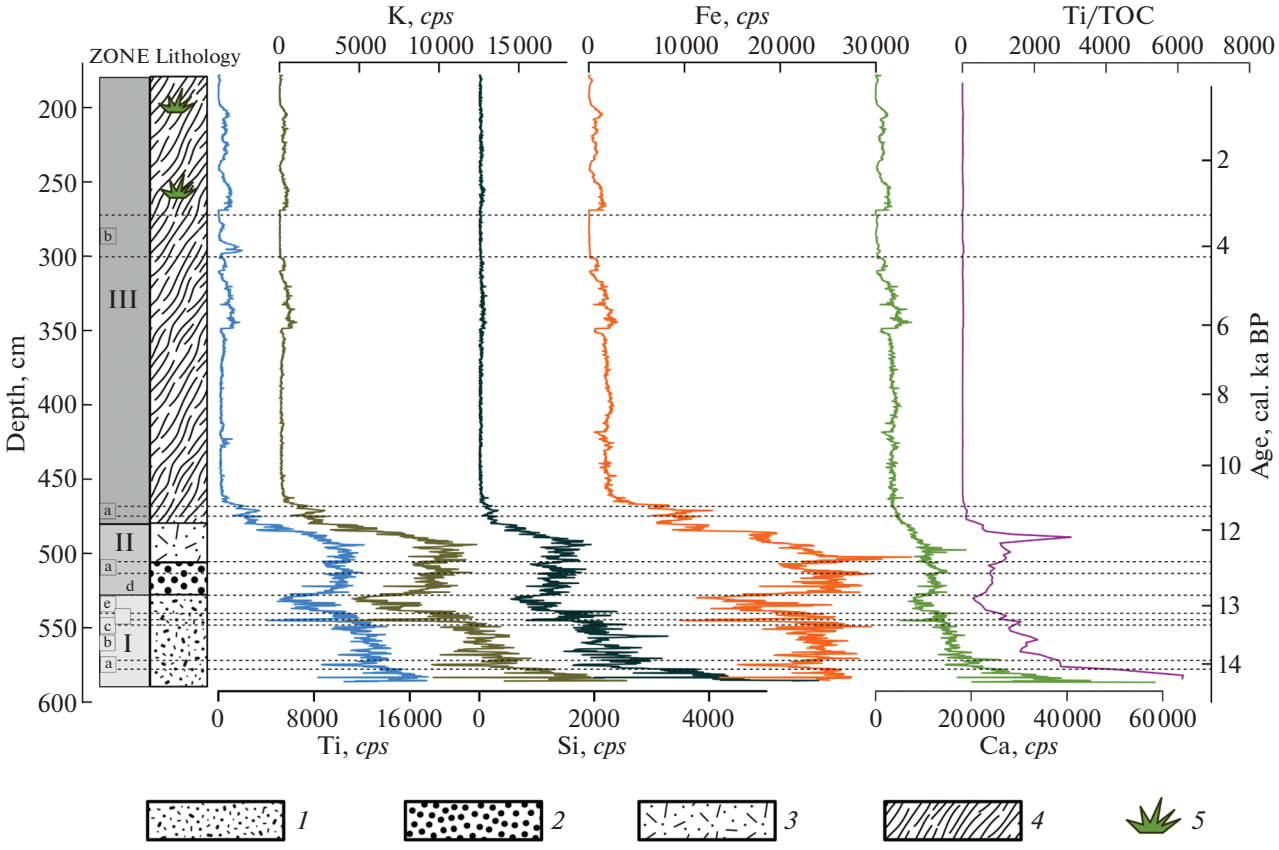

Fig. 3. Lithology and vertical distribution of Ti, K, Si and Fe content in Lake Beloye sediments. Elements content is in *cps* (counts per second). Age axis was built using age-depth modeling in rBacon. *1* – laminated sandy silt, *2* – sandy silt with organic matter, *3* – silt with organic matter, *4* – organic muds, *5* – plant fossils.

Рис. 3. Литология и вертикальное распределение содержания Ti, K, Si и Fe в отложениях оз. Белого. Элементный состав указывается в *cps* (количество импульсов в секунду). Хронологическая шкала построена с использованием функции возрастного моделирования в rBacon. *1* – слоистый опесчаненный алеврит, *2* – опесчаненный алеврит с органикой, *3* – алеврит с органикой, *4* – органогенные илы, *5* – растительные макроостатки.

depth 419–389 cm authigenic minerals (mostly goethite) content increases rapidly up to 33%. Further upcore micas and clay silicates (chlorite, kaolinite) take second place after quartz in the relative abundance of minerals, each group respectively equaling by 15–20%. Carbonates (dolomite and sometimes calcite) and hypsum are recorded sparsely (around 3–4%) and only in the bottom of the studied sediment sequence (depth interval 587–495 cm).

4.7. Principal component analysis (PCA). Two major components were distinguished as a result of the PCA, which were used to explain up to 83.1% of the whole variation. Component 1 (axis 1 in the fig. 6) embraces 73.5% of the variation, and it is mostly influenced by proxies Si, Ti, K, Fe, Ca content and χ, on the one side, which contribute by 11–12% of weight each. On the other side, TOC and WC show highest negative correlation with the mentioned proxies (11–11.5% of weight). Component 2 (axis 2 in the fig. 6) is almost completely determined by the weight of Si/Ti and Mn/Fe (60 and 30% respectively).

4. DISCUSSION AND INTERPRETATION

4.1. Geochemistry as a basement for chronostratigraphical subdivision. Silicon, potassium, titanium and iron are known to be geochemically stable and conservative elements in most environments (Boës et al., 2011; Davies et al., 2015). Although many various applications are known for Si, K, Ti, Fe appearance in sediments (i.e. redox alterations, bioproductivity changes, leaching from soils in the catchment etc.) (Mackereth, 1966; Engstrom, Wright, 1984; Boyle, 2001), it is commonly taken that these elements are used as proxies for weathering rate and allochtonous detritus inputs into the lake (Paleolimnology..., 2003; Davies et al., 2015). Linkage of these elements records in the Lake Beloye sediments with physical weathering intensity is also confirmed by the TOC variation, which was found to be inverse to the lithogenic elements accumulation. TOC is widely used in palaeolimnology as a direct proxy for lacustrine and terrestrial productivity, i.e. an onset of milder (or warmer) climatic conditions (Paleolimnology..., 2003). TOC

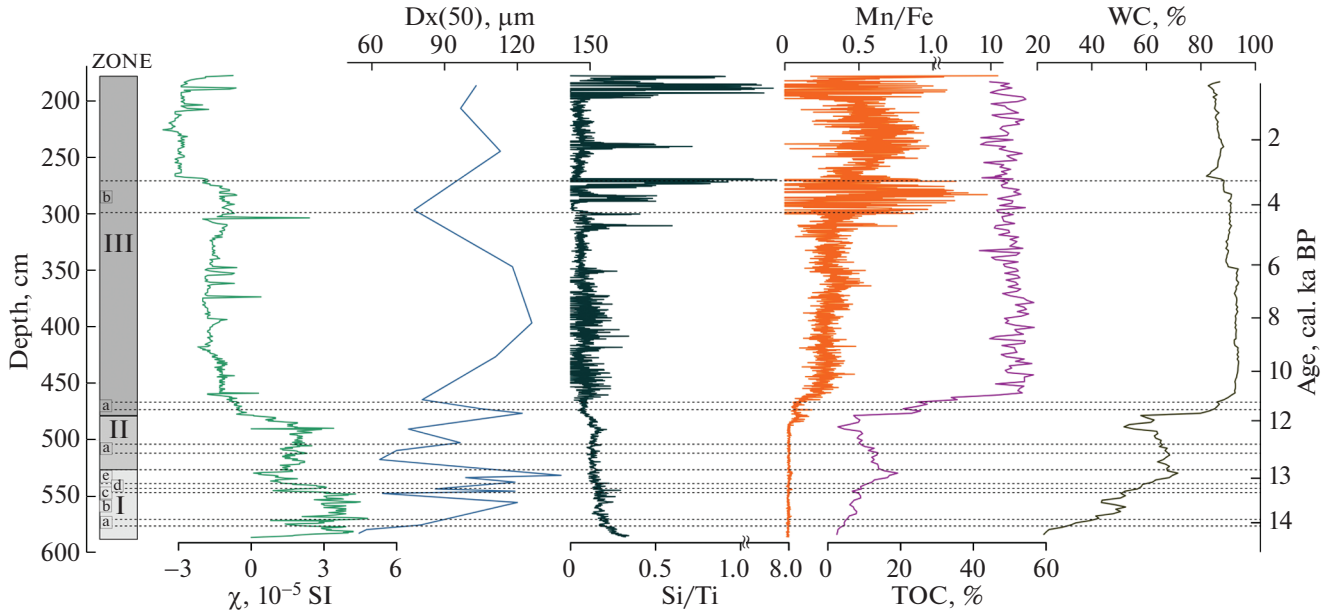

Fig. 4. Vertical distribution of magnetic susceptibility (χ), grain-size (Dx(50)), Si/Ti and Mn/Fe, total organic carbon (TOC) content and water content (WC) in the Lake Beloye sediments. Age axis was built using age-depth modelling in rBacon.

Рис. 4. Вертикальное распределение значений магнитной восприимчивости (χ), гранулометрического состава (Dx(50)), Si/Ti и Mn/Fe общего органического углерода (TOC) и содержания воды (WC) в отложениях оз. Белого. Хронологическая шкала построена с использованием функции возрастного моделирования в rBacon.

reflects even more distinctive palaeoclimatic signal when investigated in deposits of oligotrophic lake systems (Levesque, Cwynar, 1994) or in archives documenting noticeable swings in productivity or lake level (Beierle, Smith, 1998). Given the inverse correlation of lithogenic elements against TOC and WC (fig. 6), the observed geochemical record represents clear evidence that alterations of sedimentation type were likely influenced by weathering regime. In turn, erosion activity in the catchment may largely depend on the palaeohydrological and palaeoclimatic oscillations, which were investigated with the use of the age-depth model (fig. 2).

4.2. Stratigraphical units of the Lake Beloye sediment sequence. The recorded oscillations were chronologically correlated with major Late-Glacial and Holocene stratigraphic subdivisions (table 2), which had been outlined with reference to the Greenlandian ice-core studies (GICC05 timescale) (Rasmussen et al., 2014) and Scandinavian lacustrine palaeoarchives (Lohne et al., 2014).

Three zones and eight sub-zones were outlined according to the observed lithological and geochemical proxies' variation, and their palaeoenvironmental interpretation (table 2). Zone I (depth 587–526 cm) includes Late-Glacial fine silts with low TOC content. Zone II (depth 526–475 cm) embraces heterogenous horizons from the last stadial period until the assumed Pleistocene-Holocene border. Zone III (475–178 cm) contains organic muds deposited during the Holocene.

In general, inputs rate of the allochtonous material derived from physical weathering was associated with Component 1 of the PCA results (fig. 6) as a main driving factor (Van der Bilt et al., 2015) to explain the variance formation.

4.2.1. Zone I: 14.0–12.8 cal. ka BP (587–526 cm). Increased χ, Ti/TOC, minerogenic elements content (Si, Ti, K, Fe) with decreased WC and TOC mark enhanced weathering rate and low bioproductivity (Mackereth, 1966; Engstrom, Wright, 1984) in the lowermost part of zone I (587–578 cm). Reduced minerogenic sedimentation during the studied Late-Glacial section was registered ~14.0 cal. ka BP (depth 578–574 cm) (subzone I-a in the fig. 3–5 and table 2) and ~13.0 cal. ka BP (interval 539–526.5 cm) (subzone I-e in the fig. 3–5 and table 2), as derived from the lithogenic elements content decrease and TOC growth (Paleolimnology..., 2003). Interstadial climate with low catchment erosion was suggested for these intervals.

Another prominent short-term decrease of the allochtonous accumulation was noticed ~13.2 cal. ka BP (subzone I-c in the fig. 3, 4), accompanied by the raised grain-size up to 119 μm and slightly enhanced frequency of the Si/Ti oscillations (fig. 4). Altogether these proxies were interpreted to indicate regular fluctuations of bioproductivity, which likely occurred under warm climate conditions (Wennrich et al., 2014).

Elevated TOC (up to 19%), decreased Ti/TOC and lithogenic elements during subzone I-e (fig. 3, 4) are

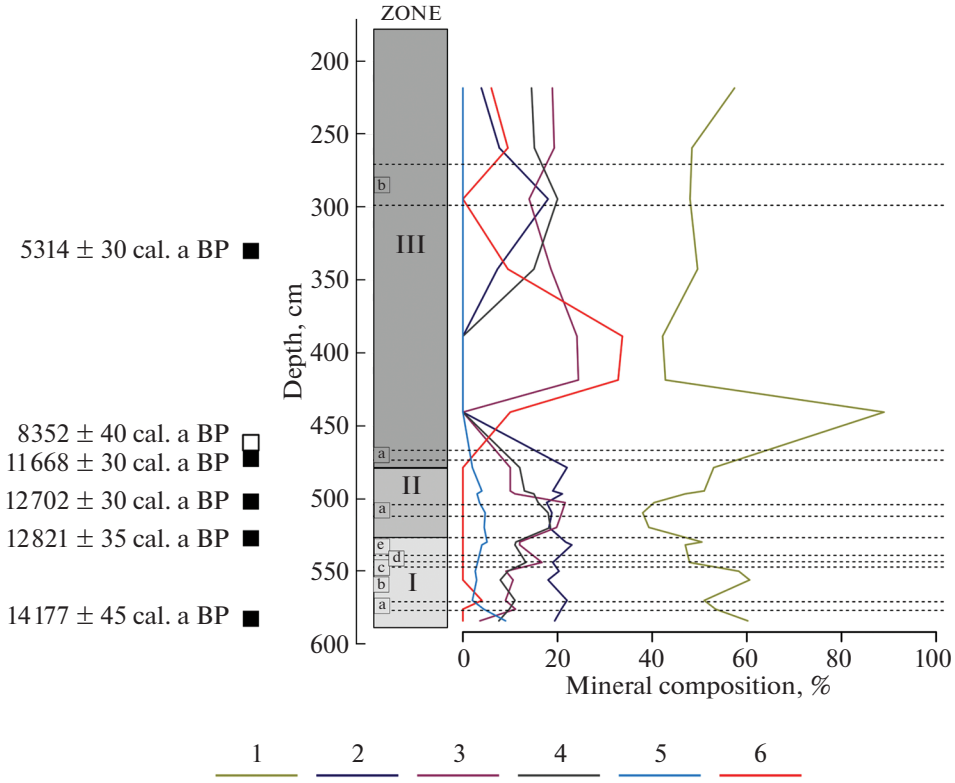

Fig. 5. Vertical distribution of the major groups of crystal minerals relative amount in the Lake Beloye sediments. 1 – quartz, 2 – feldspar minerals (albite, orthoclase, microcline, anorthite), 3 – micas (muscovite), 4 – layered silicates (chlorite, kaolinite, talc), 5 – calcite, dolomite, hypsum, 6 – authigenic minerals (goethite, pyrite, epsomite). Black squares stand for the calibrated age values obtained with AMS^{14}C dating. White square stands for the age value excluded from the age-depth model during processing in rBacon.

Рис. 5. Вертикальное распределение относительного количества основных групп кристаллических минералов в отложениях оз. Белого. 1 – кварц, 2 – полевые шпаты (альбит, ортоклаз, микроклин, анортит), 3 – слюды (мусковит), 4 – слоистые силикаты (хлорит, каолинит, тальк), 5 – кальцит, доломит, гипс, 6 – аутигенные минералы (гётит, пирит, эпсомит). Черными квадратами обозначены калиброванные значения возраста, полученные с помощью AMS^{14}C-датирования. Белым квадратом обозначено значение возраста, исключенное из возрастной модели во время моделирования в rBacon.

presumed to indicate a warming event, which chronologically correspond with the second part of the Allerød interstadial and with the stage GI-1a (Rasmussen et al., 2014).

4.2.2. Zone II: 12.8 – 11.7 cal. ka BP (525–482 cm). Sustainable growth of the lithogenic elements, χ and noticeable decrease of TOC content to 2.8% are recorded during the period starting from ~12.8 cal. ka BP (lowermost border of zone II, figs. 3–4). Apart from the proxies mentioned above, median grain-size values shift to silt fraction typically indicates water level rise (Menking, 1997). These proxies mark the abrupt shift of the sedimentation regime to that of cold stadial conditions (Kylander et al., 2013). The onset and the end of the outlined period are in good agreement with the boundaries of Younger Dryas (Lohne et al., 2014; Velichko et al., 2017) and the stage GS-1 (Rasmussen et al., 2014). Minor drop of Ti, K, Si and Fe content in the middle of zone II (subzone II-a in the fig. 3, table 2) indicates decreased weathering rate than during the rest of zone II. Similar observations were made for the bottom sediments of several North American lakes (Yu, Eicher, 1998).

4.2.3. Zone III: < 11.7 cal. ka BP (481 – 178 cm). Zone III exhibits a prominent shift in lithology, elemental composition and organic matter content in the sediments. Major palaeohydrological alterations during zone III were traced with the use of bioproductivity proxies (TOC, Si/Ti, Mn/Fe), which were interpreted to had been influenced by changes of the lake depth and redox conditions (Component 2 in the fig. 6).

The drastic change of the sedimentation regime was registered in the Lake Beloye sediments ~11.7 cal. ka BP, which is expressed in TOC increase up to 25% and simultaneous decline of the lithogenic elements content. The corresponding horizon (481–474 cm) well coincides chronologically with the lower Holocene border (Lohne et al., 2014; Rasmussen et al., 2014; Mangerud, 2021). Sporadic well-preserved *Pe-*

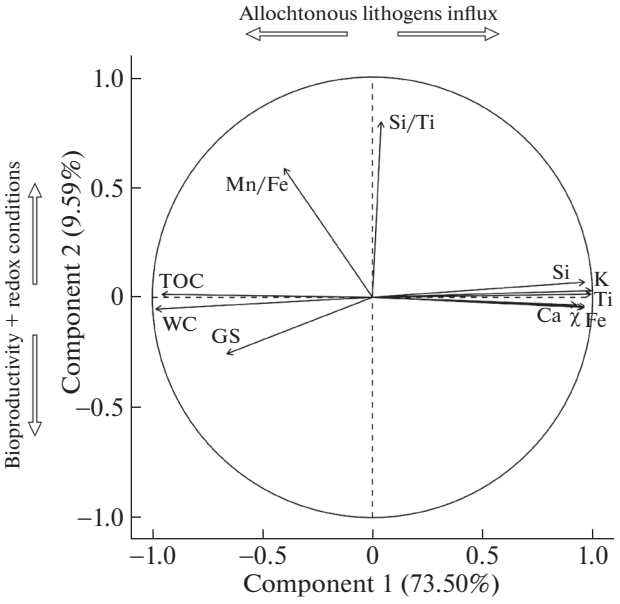

Fig. 6. Principal component analysis (PCA) biplot, calculated for 11 chemical and physical proxies. Missing values were modeled for TOC, WC, GS and χ rows with the use of missMDA package in R (Husson, Josse, 2020). Maximum circle range corresponds to the maximal vector contribution into the variance.

Рис. 6. Диаграмма по результатам анализа методом главных компонент (PCA), выполненного для 11 химических и физических показателей. Пропущенные значения были смоделированы для TOC, WC, гранулометрического состава (GS) и χ в пакете missMDA в R (Husson, Josse, 2020). Максимальный радиус окружности соответствует максимальному весу показателей в вариации.

diastrum boryanum fossils found in the material dated 11.4–11.7 cal. ka BP give evidence for the onset of warming and appearance of the algae in the relatively shallow cold-water reservoir (Jankovská, Komárek, 2000).

Carbonate minerals (dolomite, calcite) and hypsum were found abundantly in the mineral fraction of Late Glacial sediments (fig. 5), presumably being eroded from the Carboniferous limestones and dolomites underlying the thin Quaternary deposits in the area (Mokrienko et al., 1976; Jones, Bowser, 1978; Igolkina, 1985a). Carbonates and hypsum disappearance from the sediments of subzone III-a implies, most importantly, an altered weathering source in the catchment. Enhanced cryogenic fracturing and aeolian activity in the Early Holocene are confirmed by the predominance of quartz and feldspar in the silt-size deposits (Mokrienko et al., 1976; Dean, 1997; Löwemark et al., 2010; Wennrich et al., 2014; Velichko et al., 2017). In particular, these grain-size and mineralogical changes give evidence for an increasingly high erosion rates recorded ~10.1 cal. ka BP, which chronologically coincides with the cooling event 10400–10200 cal. a BP previously revealed in the lacustrine deposits of the Karelian Isthmus (Subetto et al., 2002).

Frequency and magnitude of Si/Ti and Mn/Fe oscillations increased significantly ~11.0 cal. ka BP (fig. 4), which was attributed to the final stage of the palaeolake level drop expressed in better oxygenation of the bottom water and raised productivity (Kylander et al., 2013; Naeher et al., 2013). Peat accumulation developed across the exposed vast plain territories and depressions in the basin of the drained palaeolake from the early Holocene (Mokrienko et al., 1976).

4.3. Palaeohydrological interpretation. Mologa-Sheksna palaeolake occupied much of the MSL during the late Pleistocene (Faustova et al., 1969; Gey, 2000) and in many ways influenced local hydroclimatic setting. Preserved lacustrine terraces were employed to investigate its bounds and evolution, still many of the terraces are not expressed in relief in the northern MSL (Khavin, 1962), and thus, cannot be used to carefully delineate the northern palaeolake margins.

Late Pleistocene palaeolacustrine evolution of the northern MSL was traced at a first approximation, using the multiproxy inorganic geochemistry methods. Stagnant ice complexes are believed to maintain in the central and northern MSL until the Late-Glacial (Mokrienko et al., 1976). Short duration and low lacustrine productivity during subzones I-a and I-c (figs. 3–5) were assumed to be influenced by the cooling effect of the stagnant ice (Krinner et al., 2004). The ultimate decay of the stagnant ice complexes was correlated with the onset of subzone I-e (second half of Allerød), as derived from the abrupt decrease of the lithogenic elements and enhanced grain-size values (Wennrich et al., 2014).

The level of Mologa-Sheksna palaeolake progressively declined after the final transgression in Younger Dryas. As the palaeolake was draining southwards, several large separate remnant reservoirs in the northern MSL appeared an estimated ~12.0 cal. ka BP, as confirmed by the interpretation of Mn/Fe values rise (fig. 4). Ultimately the lake level reached its up-to-date position after the series of drops ~11.7 and ~11.0 cal. ka BP, according to the enhanced water oxygenation and organic sedimentation regime onset typical for a minor relic lake, as derived from Mn/Fe and Si/Ti variations respectively (Naeher et al., 2013).

A series of abrupt palaeohydrological and trophic changes in lake Beloye are observed from ~4.2 cal. ka BP (subzone III-b in the figs. 3, 4). Mn/Fe and Si/Ti visible peaks at depth 300–269 cm indicate good bottom oxygenation and several bioproductivity bursts, which lasted until ~3.2 cal. ka BP. As Mokrienko et al. (1976) assumed, lacustrine deposits of Atlantic age of Lozskoye and Azatskoye lakes (northern Mologa-Suda lowland) could had been largely eroded in the early Subboreal, and this could possibly affect the observed geochemical proxies' variation in the Lake Beloye sediments.

Table 2. Subdivision of the Lake Beloye sediment sequence as inferred from geochemical variation
Таблица 2. Структурные и стратиграфические подразделения, выделенные в колонке оз. Белого на основе анализа вариации геохимических показателей

Sub-zone	Depth, cm	Age, cal. ka BP	Proxy	Interpretation	Stratigraphical correspondence
Zone I (587–526 cm) ~14.0–12.8 cal. ka BP					
Deposition was largely influenced by influx of clastic detrital material (enhanced content of Ti, K, Si, Fe and low TOC values). Long-lasting degradation of the stagnant ice fields presumably caused low bioproductivity and intensive physical weathering for the most of the Late Glacial					
I-a	578–574	~14.0	Drastic drop of Si, K, Ti, Fe. Low TOC and Mn/Fe	Low hydrological activity and allochtonous inwash. Deep-water (anoxic) facies	Bølling, stage GI-1e
I-b	574–547	~13.5	High Si, K, Ti, Fe. Low TOC	Enhanced minerogenic sedimentation	Older Dryas, stage GI-1d
I-c	547–544	~13.2	Abrupt decrease of Si, K, Ti, Fe. GS rise to 119 μm	Short-term warming, halted minerogenic inwash possibly due to decay of the stagnant ice fields	Allerød, stage GI-1c1
I-d	544–539	~13.1	Low TOC (9%) and GS (86 μm), high Si, K, Ti, Fe	Short-term cooling. Allochtonous inwash prevails	Allerød, stage GI-1b, Intra-Allerød Cold Period (Gerzensee-Killarney Oscillation)
I-e	539–526.5	~13.0	Low Si, K, Ti, Fe, elevated TOC (19%), high GS values (138 μm)	Most prominent pause of minerogenic inwash. The onset of warm climate and lake level drop	Allerød, stage GI-1a
Zone II (526–482 cm) ~12.8–11.7 cal. ka BP					
Cold climate with high weathering rate and lake level rise are marked by simultaneous increase of Ti, K, Si, Fe content, synchronous TOC decline and a grain-size offset to silt fraction. The cold period margins are in good agreement with the duration of Younger Dryas and stage GS-1					
II-a	512–504	~12.7	Minor drop of Ti, K, Si and Fe	Declined physical weathering	Younger Dryas, GS-1
Zone III (482–178 cm) <11.7 cal. ka BP					
Rapid TOC increase (50%), abrupt decline in minerogenic accumulation and authigenic minerals formation indicate an unprecedent lacustrine bioproductivity growth, coinciding with the generally accepted Holocene onset along with the large palaeolake level fall, which ultimately drained by ~11.0 cal. ka BP (Preboreal)					
III-a	474–468	<11.5	High Ti, K, Fe, Si; Mn/Fe and TOC halt	Enhanced weathering rates and low TOC may indicate a slight cooling	Preboreal
III-b	300–269	~4.2–3.2	Series of Mn/Fe and Si/Ti peaks	Hydrological and trophic alterations	Middle Holocene

5. CONCLUSION

Pronounced palaeohydrological and sedimentological changes of the minor basin were outlined and carefully correlated with global chronostratigraphic schemes for the Late-Glacial and the Holocene. Multiproxy approach of combined organic and inorganic geochemical and mineralogical methods, enforced with the accurate age control, enabled to conclude the following:

1) Uninterrupted lacustrine deposits represent one of the best palaeoarchives for building a detailed palaeoenvironmental reconstruction, if commenced comprehensively, with the use of high-resolution scanning methods, physical properties measurements and a proper age control. Geochemical proxies investigated in the Lake Beloye sediments are indirectly linked with the regional palaeoclimatic conditions, giving evidence for the transport and accumulation of

mineral matter in the dynamic lacustrine and glaciolacustrine environments.

2) Low weathering rate and enhanced lacustrine bioproductivity, correlated with warmer climatic conditions, were revealed in the northern MSL ~14.0 cal. ka BP and ~13.0 cal. ka BP, and chronologically correspond to Bølling (stage GI-1e) and Allerød (stages GI-1c3 – GI-1a) (table 2) (Lohne et al., 2014; Rasmussen et al., 2014).

3) Interval of the sediment sequence, dated as 12.8–11.7 cal. ka BP, was corresponded to Younger Dryas cooling (table 2) by its geochemical signal and major mineral composition.

4) The Pleistocene/Holocene boundary in the Lake Beloye sediments was attributed to the layer dated ~11.7 cal. ka BP (table 2). From the end of Younger Dryas (~12.1 cal. ka BP) the overall glacial termination course featured a series of oscillations, which were interpreted as short-term warming and cooling events alteration.

5) Periods of increased detritus input rate, high lake level and low productivity were captured in the Lake Beloye sediments ~13.7 cal. ka BP, ~13.1 cal. ka BP and ~11.5 cal. ka BP, which were palaeoclimatically and chronologically associated with the cooling events Older Dryas (GI-1d stage), Gerzensee-Killarney Oscillation (GI-1b stage) (Levesque et al., 1993; Rasmussen et al., 2014) and Preboreal oscillation (11.4 ka BP event) (Björck et al., 1997; Rasmussen et al., 2014) respectively (table 2).

6) Stages of the Mologa-Sheksna palaeolake level decrease were traced with the use of palaeoredox and bioproductivity proxies (Mn/Fe and Si/Ti). After a brief lake level drop in Allerød, transgression occurred during Younger Dryas, and several step-wise lake level declines were recorded ~12.0 cal. ka BP, ~11.7 cal. ka BP and, ultimately, ~11.0 cal. ka BP.

Late-Glacial to Middle Holocene Sedimentation in Lake Beloye (Vologda Region, Northwestern Russia)

D. O. Sadokov[a,b,#], T. V. Sapelko[c], M. Melles[d], and G. B. Fedorov[b,e]

[a] *Darwin State Nature Biosphere Reserve, Cherepovets, Russia*
[b] *St. Petersburg State University, Institute of Earth Sciences, St. Petersburg, Russia*
[c] *Institute of Limnology of the RAS, SPC RAS, St. Petersburg, Russia*
[d] *University of Cologne, Institute of Geology and Mineralogy, Cologne, Germany*
[e] *Arctic and Antarctic Research Institute, St. Petersburg, Russia*
[#] *E-mail: dmitriisadokov@gmail.com*

Lake sediments of the northern Mologa-Sheksna Lowland were for the first time studied using high-resolution x-ray fluorescence scanning and AMS dating, supplemented with x-ray diffraction, total organic carbon, grain-size and magnetic susceptibility measurements. The combined results revealed sedimentation type changes during the Late Glacial and Early Holocene, which were associated with the proportions of allogenic and authigenic material in the deposits. Short-lived periods of low allogenic activity were registered ~14.0 cal. ka BP and ~13.0 cal. ka BP, interrupted by episodes of enhanced minerogenic input and low organic accumulation ~13.7, ~13.1 and ~11.5 cal. ka BP. The outlined intervals correspond with the Late-Glacial climatostratigraphic units of the North Atlantic region. The beginning of the organic sedimentation ~11.7 cal. ka BP indicates climatic warming of the Early Holocene. During the Younger Dryas and Early Holocene, until ~11.0 cal. ka BP, the sedimentation was furthermore influenced by the lake-level changes.

Keywords: lacustrine sedimentation, geochemistry, Allerød, Younger dryas

ACKNOWLEDGMENTS

Fieldwork was supported by RFBR (project No. 19-35-90026) and conducted on the basis of the joint scientific work between Darwin Nature Biosphere reserve and Institute of Limnology RAS SPC RAS in frames of scientific topics approved in Darwin Nature Biosphere reserve ("Palaeogeography of the Mologa-Sheksna lowland", 2018; "Dynamics of the natural complexes of Darwin State Nature Biosphere reserve", 2019, 2020; "Evolution and the current state of the landscapes of Darwin State Nature Biosphere reserve", 2021) and in Institute of Limnology RAS SPC RAS (Topic No. 0154-2019-0001).

Laboratory and analytical work was performed with the support of Ministry of Science and Higher Education of the Russian Federation, Agreement No. 075-15-2022-236. X-ray fluorescence scanning, total organic carbon and water content measurements were performed in the Laboratory of the Quaternary geology work group, Institute of Geology and Mineralogy, University of Cologne (Cologne, Germany). Quantitative X-ray fluorescence and X-ray diffraction studies were performed in the Centre for X-Ray Diffraction Studies, St. Petersburg State University (St. Petersburg, Russia). Grain size measurements were performed in the Centre for Innovative Technologies of Composite Nano-

materials, St. Petersburg State University (St. Petersburg, Russia). AMS dating was conducted in the Laboratory of radiocarbon dating and electronic microscopy, Institute of Geography, Russian Academy of Sciences (Moscow, Russia). Optical studies were conducted in the Centre for Microscopy and Microanalysis, St. Petersburg State University (St. Petersburg, Russia).

REFERENCES

Astakhov V., Shkatova V., Zastrozhnov A., and Chuyko M. Glaciomorphological map of the Russian Federation *Quat. Int.* 2016. Vol. 420. P. 4–14. https://doi.org/10.1016/j.quaint.2015.09.024

Auslender V.G. *Istoriya razvitiya Mologo-Sheksninskogo ozera*. (History of the Mologa-Sheksna lake development). *Materialy I simpoziuma po istorii ozer Severo-Zapada SSSR. "Istoriya ozer SSSR"*. L.: Geograficheskoye obschestvo SSSR (Publ.), 1967. P. 201–209. (in Russ.)

Beierle B. and Smith D.G. Severe drought in the early Holocene (10,000-6800 BP) interpreted from lake sediment cores, southwestern Alberta, Canada. *Palaeogeogr. Palaeoclimatol. Palaeoecol.* 1998. Vol. 140. P. 75–83. https://doi.org/10.1016/S0031-0182(98)00044-3

Björck S., Rundgren M., Ingólfsson O., and Funder S. The Preboreal oscillation around the Nordic seas: terrestrial and lacustrine responses *J. Quat. Sci.* 1997. Vol. 12. No. 6. P. 455–465. https://doi.org/10.1002/(SICI)1099-1417(199711/12)12:6<455::AID-JQS316>3.0.CO;2-S

Blaauw M. and Christen J.A. rbacon: Age-depth modelling using Bayesian statistics. R package version 2.3.9.1. 2019. URL: https://cran.r-project.org/web/packages/rbacon/index.html (Accessed 15.01.2021)

Boës X., Rydberg J., Martinez-Cortizas A., Bindler R., and Renberg I. Evaluation of conservative lithogenic elements (Ti, Zr, Al, and Rb) to study anthropogenic element enrichments in lake sediments. *J. Paleolimnol.* 2011. Vol. 46. P. 75–87. https://doi.org/10.1007/s10933-011-9515-z

Boyle J.F. Inorganic geochemical methods in palaeolimnology. Tracking environmental change using lake sediments (Physical and geochemical methods). Vol. 2. W.M. Last and J.P. Smol. Ed. New-York, Boston, Dordrecht, London, Moscow: Kluwer Academic Publishers (Publ.), 2001. P. 83–141. https://doi.org/10.1007/0-306-47670-3_5

Chebotaryova N.S. *Granitsa maksimal'nogo rasprostraneniya poslednego lednikovogo pokrova i nekotorye problemy stratigrafii i paleogeografii verkhnego pleistotsena severo-zapada evropeiskoi chasti SSSR.* (Last glaciation extent border and problems of the upper Pleistocene stratigraphy and paleogeography of the European part of USSR). *Trudy Komissii po izucheniyu chetvertichnogo perioda*. Vol. 19. *Voprosy stratigrafii i paleogeografii chetvertichnogo perioda (antropogena)* (Questions of stratigraphy and paleogeography of the Quaternary (Antropogene)). 1962. P. 148–169. (in Russ.)

Davies S.J., Lamb H.F., and Roberts S.J. Micro-XRF core scanning in palaeolimnology: recent developments (Micro-XRF studies of sediment cores: applications of a non-destructive tool for the environmental sciences). Developments in palaeoenvironmental research. Vol. 17. I.W. Croudace and R.G. Rothwell. (Eds.). Dordrecht, Heidelberg, New-York, London: Springer (Publ.). 2015. P. 189–226. https://doi.org/10.1007/978-94-017-9849-5_7

Dean W.E. Rates, timing, and cyclicity of Holocene eolian activity in north-central United States: evidence from varved lake sediments. *Geology.* 1997. Vol. 25. No. 4. P. 331–334. https://doi.org/10.1130/0091-7613(1997)025<0331:RTACOH>2.3.CO;2

Engstrom D.R. and Wright H.E.Jr. Chemical stratigraphy of lake sediments as a record of environmental change. Lake sediments and environmental history. E.Y. Haworth and J.W.G. Lund. Ed. Leicester: Leicester University Press (Publ.), 1984. P. 11–68.

Faustova M.A., Auslender V.G., Grichuk V.P., Smirnov V.I., and Malgina E.A. *Degradatsiya valdaiskogo oledeneniya i pozdnelednikovaya istoriya Baltiiskogo i Belogo morei. Vologodskaya oblast'*.(Degradation of the valdai glaciation and late-glacial history of the Baltic and White seas. Vologda region). *Poslednii lednigovyi pokrov na severo-zapade Evropeiskoi chasti SSSR.* (Last glacial cover on the North-West of the European part of USSR). I.P. Gerasimov (Ed.). M.: Nauka (Publ.), 1969. P. 192–214. (in Russ.)

Gey V.P. *Istoriya razvitiya krupnykh ozer s kontsa srednego neopleistotsena do golotsena na territorii Vologodskoi i smezhnykh oblastei* (History of the large lakes from the end of the middle Neopleistocene to Holocene in Vologda region and adjacent regions). *Materialy mezhdunarodnogo simpoziuma "Problemy stratigrafii chetvertichnykh otlozheniy i kraevye lednikovye obrazovaniya Vologodskogo regiona (severo-zapad Rossii)*. Kirillov: GEOS (Publ.), 2000. P. 65–70. (in Russ.)

Hughes A.L.C., Gyllencreutz R., Lohne I.S., Mangerud J., and Svendsen J.I. The last Eurasian ice sheets – a chronological database and time-slice reconstruction // DATED-1. *Boreas*. 2016. Vol. 45. No. 1. P. 1–45. https://doi.org/10.1111/bor.12142

Husson F. and Josse J. missMDA: Handling Missing Values with Multivariate Data Analysis. R package version 1.18. 2020. URL: https://cran.r-project.org/web/packages/missMDA/index.html (Accessed 28.02.2021)

Husson F., Josse J., Le S., and Mazet J. FactoMineR: Multivariate Exploratory Data Analysis and Data Mining. R package version 1.42. 2019. URL: https://cran.r- project.org/web/packages/FactoMineR/index.html (Accessed 09.02.2021)

Igolkina N.S. (Ed.). *Geologicheskaya karta. Maschtab 1:200 000. List O-36-VI.* (Geological map on the territory of sheet O-36-VI (scale 1:200000)). L.: VSEGEI (Publ.), 1985a. (in Russ.)

Igolkina N.S. (Ed.). *Karta chetvertichnykh obrazovanii. Maschtab 1:200 000. List O-36-VI.* (Map of Quaternary formations on the territory of sheet O-36-VI (scale 1:200000)). L.: VSEGEI (Publ.), 1985b. (in Russ.)

Jankovská V. and Komárek J. Indicative Value of *Pediastrum* and other coccal green algae in palaeoecology. *Folia*

Geobot. 2000. Vol. 35. P. 59–82.
https://doi.org/10.1007/BF02803087

Jones B.F. and Bowser C.J. The mineralogy and related chemistry of lake sediments. (Lakes – Chemistry, Geology, Physics). A. Lerman. Ed. New-York: Springer (Publ.), 1978. P. 179–235.
https://doi.org/10.1007/978-1-4757-1152-3_7

Kassambara A. and Mundt F. factoextra: Extract and Visualize the Results of Multivariate Data Analyses. R package version 1.0.7. 2020. URL: https://cran.r-project.org/web/packages/factoextra/index.html (Accessed 25.03.2021)

Khavin Ye.I. *Chetvertichnye otlozheniya severnoi poloviny Mologo-Sheksninskoi niziny* (Quaternary deposits of the northern Mologa-Sheksna lowland). *Voprosy stratigrafii chetvertichnykh otlozheni- Severo-Zapada Evropeiskoi chasti SSSR.* (Questions of the Quaternary sediments stratigraphy of the North-West of the European part of USSR). M.A. Lavrova, A.P. Faddeeva, A.P. Zhingarev-Dobroselskiy (Eds.). L: Gosudarstvennoye nauchno-tekhnicheskoye izdatelstvo neftyanoi i gorno-toplivnoi literatiry. Leningradskoye otdeleniye (Publ.), 1962. P. 109–124. (in Russ.)

Krinner G., Mangerud J., Jakobsson J., Crucifix M., Ritz C. and Svendsen J.I. Enhanced ice sheet growth in Eurasia owing to adjacent ice dammed lakes. *Nature*. 2004. Vol. 427. No. 6973. P. 429–432.
https://doi.org/10.1038/nature02233

Kylander M.E., Klaminder J., Wohlfarth B., and Löwemark L. Geochemical responses to paleoclimatic changes in southern Sweden since the late glacial: the Hässeldala Port lake sediment record. *J. Paleolimnol.* 2013. Vol. 50. No. 1. P. 57–70.
https://doi.org/10.1007/s10933-013-9704-z

Levesque A.J. and Cwynar L.C. A multiproxy investigation of Late-Glacial climate and vegetation change at Pine Ridge Pond, Southwest New Brunswick, Canada. *Quat.* 1994. Vol. 42. Is. 3. P. 316–327.
https://doi.org/10.1006/qres.1994.1082

Levesque A.J., Mayle F.E., Walker I.R., and Cwynar L.C. A previously unrecognized late-glacial cold event in eastern North America. *Nature.* 1993. Vol. 361. No. 6413. P. 623–626.
https://doi.org/10.1038/361623a0

Lohne Ø.S., Mangerud J., and Birks H.H. IntCal13 calibrated ages of the Vedde and Saksunarvatn ashes and the Younger Dryas boundaries from Kräkenes, western Norway. *J. Quat. Sci.* 2014. Vol. 29. No. 5. P. 506–507.
https://doi.org/10.1002/jqs.2722

Löwemark L., Chen H.-F., Yang T.-N., Kylander M., Yu E.-F., Hsu Y.-W., Lee T.-Q., Song S.-R., and Jarvis S. Normalizing XRF-scanner data: A cautinoary note on the interpretation of high-resolution records from organic-rich lakes. *J. Asian Earth Sci.* 2010. Vol. 40. No. 6. P. 1250–1256.
https://doi.org/10.1016/j.jseaes.2010.06.002

Lunkka J., Saarnisto M., Gey V., Demidov I., and Kiselova V. 2001 Extent and age of the Last Glacial Maximum in the southeastern sector of the Scandinavian Ice Sheet *Glob. Planet. Change*. 2001. Vol. 31. No. 1–4. P. 407–425.
https://doi.org/10.1016/S0921-8181(01)00132-1

Mackereth F.J.H. Some chemical observations on post-glacial lake sediments. *Philos. Trans. R. Soc. Lond. B, Biol. Sci.* Series B. Biological Sciences. 1966. Vol. 250. No. 765. P. 165–213.
https://doi.org/10.1098/rstb.1966.0001

Maksutova N.K. and Vorobyov G.A. *Landshaftnoe raionirovanie Vologodskoi oblasti.* (Lanscape zones of Vologda region). 2007. *Priroda Vologodskoi oblasti* (Nature of Vologda region). G.A. Vorobyov (Ed.). Vologda: Izdatelskiy Dom Vologazhanin (Publ.), P. 301–328. (in Russ.)

Mangerud J. The discovery of the Younger Dryas, and comments on the current meaning and usage of the term. *Boreas.* 2021. Vol. 50. No. 1. P. 1–5.
https://doi.org/10.1111/bor.12481

Mangerud J., Jakobsson M., Alexanderson H., Astakhov V., Clarke G.K.C., Henriksen M., Hjort C., Krinner G., Lunkka J.P., Möller P., Murray A., Nikolskaya O., Saarnisto M., and Svendsen J.I. Ice-dammed lakes, rerouting of the drainage of Northern Eurasia during the last glaciation *Quat. Sci. Rev.* 2004. Vol. 23. No. 11–13. P. 1313–1332.
https://doi.org/10.1016/j.quascirev.2003.12.009

Menking K.M. Climatic signals in clay mineralogy and grain-size variations in Owens Lake core OL-92, southeast California. An 800,000-year Paleoclimatic Record from Core OL-92, Owens Lake, Southeast California. G.I. Smitrh and J.L. Bischoff (Eds.). *Geol. Soc. Am. Spec. Pap.* 1997. Vol 317. P. 37–48.
https://doi.org/10.1130/0-8137-2317-5.25

Mokrienko Z.M., Aleksandrova N.A., Auslender V.G., Poluektov L.N., Chervakov Yu.I., and Borovikova N.A. *Otchet o gruppovoi kompleksnoi geologo-gidrogeologicheskoi s'emke masshtaba 1:200000 basseina r. Sudy Vologodskoi oblasti (1972–76 gg.).* (Report on the complex geological survey in the r. Suda basin (Vologda region) in scale 1:200000 (1972–76)). Vol. 1. No. 1. L: VSEGEI (Publ.), 1976. 269 p. (in Russ.)

Moskvitin A.I. *Mologo-Sheksninskoe mezhlednikovoe ozero.* (Mologa-Sheksna interglacial lake). 1947. *Trudy Instituta geologicheskikh nauk*. Vol. 88. Seriya Geologicheskaya. No. 26. P. 5–18. (in Russ.)

Naeher S., Gilli A., North R.P., Hamann Y., and Schubert C.J. Tracing bottom water oxygenation with sedimentary Mn/Fe ratios in Lake Zurich, Switzerland. *Chem. Geol.* 2013. Vol. 352. No. 16. P. 125–133.
https://doi.org/10.1016/j.chemgeo.2013.06.006

Paleolimnology: the history and evolution of lake systems. A.S. Cohen. New-York: Oxford University Press (Publ.), 2003. 500 p.

Pozdnechetvertichnaya istoriya krupnykh ozer i vnutrennikh morei Vostochnoi Evropy (Late Quaternary history of the large lakes and inland seas of the Eatern Europe). Kvasov D.D. Martinson G.G. and Davydova N.N. (Eds.). L.: Nauka (Publ.), 1974. 278 p. (in Russ.)

Rasmussen S.O., Bigler M., Blockley S.P., Blunier T., Buchardt S.L., Clausen H.B., Cvijanovic I., Dahl-Jensen D., Johnsen S.J., Fischer H., Gkinis V., Guillevic M., Hoek W.Z., Lowe J.J., Pedro J.B., Popp T., Seierstad I.K.,

Steffensen J.P., Svensson A.M., Vallelonga P., Vinther B.M., Walker M.J., Wheatley J.J., and Winstrup M. A stratigraphic framework for abrupt climatic changes during the Last Glacial period based on three synchronized Greenland ice-core records: refining and extending the INTIMATE event stratigraphy. *Quat. Sci. Rev.* 2014. Vol. 106. No. 15. P. 14–28. https://doi.org/10.1016/j.quascirev.2014.09.007

Reimer P., Austin W.E.N., Bard E., Bayliss A, Blackwell P.G., Ramsey C.B., Butzin M., Edwards R.L., Friedrich M., Grootes P.M., Guilderson T.P., Hajdas I., Heaton T.J., Hogg A., Kromer B., Manning S.W., Muscheler R., Palmer J.G., Pearson C., van der Plicht J., Reimer R.W., Richards D.A., Scott E.M., Southon J.R., Turney C.S.M., Wacker L., Adolphi F., Büntgen U., Fahrni S., Fogtmann-Schulz A., Friedrich R., Köhler P., Kudsk S., Miyake F., Olsen J., Sakamoto M., Sookdeo A., and Talamo S. The IntCal20 Northern Hemisphere radiocarbon age calibration curve (0–55 cal kB). *Radiocarbon*. 2020. Vol. 62. No. 4. P. 725–757. https://doi.org/10.1017/RDC.2020.41

Saarnisto M. and Saarinen T. Deglaciation chronology of the Scandinavian Ice Sheet from the lake Onega basin to the Salpausselkä end moraines. *Glob. Planet. Change*. 2001. Vol. 31. No. 1–4. P. 387–450. https://doi.org/10.1016/S0921-8181(01)00131-X

Sapelko T.V., Subetto D.A., and Sevastyanov D.V. *Vodlozero: Istoriya razvitiya* (Vodlozero: History of development). 2006. *Materialy nauchno-prakticheskoi konferentsii "Vodlozerskie chteniya. Estestvennoonauchnye i gumanitarnye osnovy prirodookhrannoi i prosvetitel'skoi deyatel'nosti na okhranyaemykh prirodnykh territoriyakh Russkogo Severa"*. Petrozavodsk: Karelian Research Centre RAS (Publ.), P. 37–44. (in Russ.)

Subetto D.A., Wohlfarth B., Davydova N.N., Sapelko T.V., Björkman L., Solovieva N., Wastegård S., Possnert G., and Khomutova V.I. Climate and environment on the Karelian Isthmus, northwestern Russia, 13000–9000 cal yrs BP. *Boreas*. 2002. Vol. 31. No. 1. P. 1–19. https://doi.org/10.1111/j.1502-3885.2002.tb01051.x

Svendsen J.I., Alexanderson H., Astakhov V.I., Demidov I., Dowdeswell J.A., Funder S., Gataullin V., Henriksen M., Hjort C., Houmark-Nielsen M., Hubberten H.W., Ingólfsson Ó., Jakobsson M., Kjær K.H., Larsen E., Lokrantz H., Lunkka J.P., Lyså A., Mangerud J., Matiouchkov A., Murray A., Möller P., Niessen F., Nikolskaya O., Polyak L., Saarnisto M., Siegert C., Spielhagen R.F., and Stein R. Late Quaternary ice sheet history of northern Eurasia. *Quat. Sci. Rev.* 2004. Vol. 23. No. 11–13. P. 1229–1271. https://doi.org/10.1016/j.quascirev.2003.12.008

Van der Bilt W.G.M., Bakke J., Vasskog K., D'Andrea W.J., Bradley R.S., and Ólafsdóttir S. Reconstruction of glacier variability from lake sediments reveals dynamic Holocene climate in Svalbard. *Quat. Sci. Rev.* 2015. Vol. 126. P. 201–218. https://doi.org/10.1016/j.quascirev.2015.09.003

Velichko A.A. and Faustova M.A. *Razvitie oledenenii v pozdnem pleistotsene. Paleoklimaty i paleolandshafty vnetropicheskogo prostranstva Severnogo polushariya. Pozdnii pleistotsen – golotsen* (Glaciations during the Late Pleistocene. Paleoclimates and paleoenvironments of extra-tropical regions of the Northern Hemisphere. Late Pleistocene – Holocene). A.A. Velichko (Ed.). M.: GEOS (Publ.), 2009. P. 32–41. (in Russ.)

Velichko A.A., Faustova M.A., Pisareva V.V., and Karpukhina N.V. History of the Scandinavian ice sheet and surrounding landscapes during Valday ice age and the Holocene. *Ice and Snow*. 2017. Vol. 57. No. 3. P. 391–415. (in Russ.). https://doi.org/10.15356/2076-6734-2017-3-391-416

Wennrich V., Minyuk P.S., Borkhodoev V., Francke A., Ritter B., Nowaczyk N.R., Sauerbrey M A., Brigham-Grette J., and Melles M. Pliocene to Pleistocene climate and environmental history of Lake El'gygytgyn, Far East Russian Arctic, based on high-resolution inorganic geochemistry data. *Climate of the Past*. 2014. Vol. 10. No. 4. P. 1381–1399. https://doi.org/10.5194/cp-10-1381-2014

Yu Z. and Eicher U. Abrupt climate oscillations during the last deglaciation in Central North America. *Science, Reports*. 1998. Vol. 282. No. 5397. P. 2235–2238. https://doi.org/10.1126/science.282.5397.2235